Pergamon

The kinetics of the oxidation of pyrite by ferric ions and dissolved oxygen: An electrochemical study

PAUL R. HOLMES and FRANK K. CRUNDWELL*

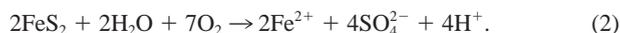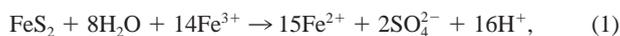Billiton Centre for Bioprocess Modelling, University of the Witwatersrand, Johannesburg, South Africa

Abstract—The dissolution of pyrite is important in the geochemical cycling of iron and sulphur, in the formation of acid mine drainage, and in the extraction of metals by bacterial leaching. Many researchers have studied the kinetics of dissolution, and the rate of dissolution has often been found to be half-order in ferric ions or oxygen. Previous work has not adequately explained the kinetics of dissolution of pyrite. The dissolution of pyrite is an oxidation-reduction reaction. The kinetics of the oxidation and reduction half-reactions was studied independently using electrochemical techniques of voltammetry. The kinetics of the overall reaction was studied by the electrochemical technique of potentiometry, which consisted of measuring the mixed potential of a sample of corroding pyrite in solutions of different compositions. The kinetics of the half reactions are related to the kinetics of the overall dissolution reaction by the condition that there is no accumulation of charge. This principle is used to derive expressions for the mixed potential and the rate of dissolution, which successfully describe the mixed potential measurements and the kinetics of dissolution reported in the literature. It is shown that the observations of half-order kinetics and that the oxygen in the sulphate product arises from water are both a direct consequence of the electrochemical mechanism. Thus it is concluded that the electrochemical reaction steps occurring at the mineral-solution interface control the rate of dissolution. Raman spectroscopy was used to analyze reaction products formed on the pyrite surface. The results indicated that small amounts of polysulphides form on the surface of the pyrite. However, it was also found that the mixed (corrosion) potential does not change over a 14-day leaching period. This indicates that even though polysulphide material is present on the surface, it does not influence the rate of the reactions occurring at the surface. Measurements of the sulphur yields as a function of electrode potential indicate that thiosulphate is not the only source of the sulphur product. *Copyright © 2000 Elsevier Science Ltd*

1. INTRODUCTION

Pyrite, FeS_2, is the most common sulphide mineral. It is found in magmatic and igneous rocks, sedimentary deposits, and hydrothermal deposits. It is a commercial source of sulphuric acid, and it is presently mined as a source of gold and cobalt, which are associated with it. However, in most cases it is a gangue mineral in metallurgical processes. Because of these factors, pyrite is often exposed to the environment by mining and metallurgical activities. The oxidation of exposed pyrite is a cause of acid drainage, an environmental problem of considerable concern. Vast sums are invested in the alleviation of acid mine drainage. In the United States, approximately $1,000,000 per day is spent on acid mine drainage (Evangelou, 1995).

The mechanism of the formation of acid mine drainage is the combination of two reactions: the oxidation of pyrite by ferric ions or oxygen and the oxidation of ferrous ions by oxygen. Pyrite dissolves by the following reactions:

$$FeS_2 + 8H_2O + 14Fe^{3+} \rightarrow 15Fe^{2+} + 2SO_4^{2-} + 16H^+, \quad (1)$$

$$2FeS_2 + 2H_2O + 7O_2 \rightarrow 2Fe^{2+} + 4SO_4^{2-} + 4H^+. \quad (2)$$

The product of these reactions, ferrous ions, is oxidized by oxygen in the following reaction (Singer and Stumm, 1970):

$$4Fe^{2+} + O_2 + 4H^+ \rightarrow 4Fe^{3+} + 2H_2O. \quad (3)$$

Thus, ferrous and ferric ions are cycled between the pyrite oxidation reaction (1) and ferrous ion oxidation reaction (3). The overall reaction generates acid, which results in environmental damage.

The kinetics and the mechanism of the oxidation of pyrite has received much attention (Lowson, 1982; Wiersma and Rimstidt, 1984; McKibben and Barnes, 1986; Luther, 1987; Moses et al., 1987; Williamson and Rimstidt, 1994). Lowson (1982) and Evangelou (1995) reviewed the kinetics of pyrite oxidation. Wiersma and Rimstidt (1984), McKibben and Barnes (1986), and Williamson and Rimstidt (1994) studied the rate of the oxidation of pyrite by ferric ions and dissolved oxygen. In general, the rate of oxidation of pyrite increases with the concentration of ferric ions, and decreases with the concentrations of ferrous and H^+ ions. Isotope studies indicate that water, rather than molecular oxygen, is the source of oxygen in the sulphate product of reactions (1) and (2) (Reedy et al., 1991; Taylor et al., 1984a, 1984b; Bailey and Peters, 1976). Wiersma and Rimstidt (1984), McKibben and Barnes (1986), and Williamson and Rimstidt (1994) proposed different empirical expressions for the rate of oxidation of pyrite. The form of the rate expression has been discussed in terms of adsorption theory (Williamson and Rimstidt, 1994) and molecular orbital theory (Moses et al., 1987).

Although an electrochemical mechanism for the oxidation of pyrite by ferric ions was discussed by McKibben and Barnes (1986) and Williamson and Rimstidt (1994), very little work on

---

* Author to whom correspondence should be addressed: School of Process and Materials Engineering, University of the Witwatersrand, Private Bag 3, Wits, 2050, South Africa (FKC@chemeng.chmt.wits.ac.za).
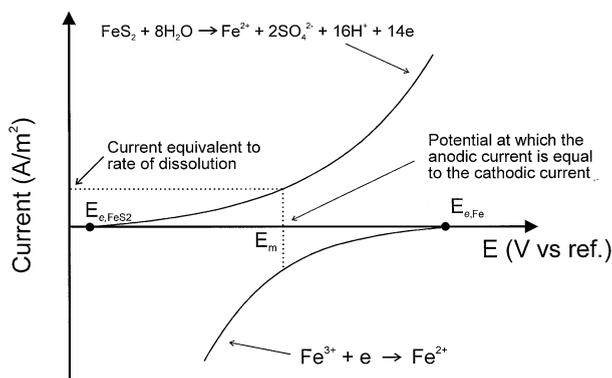
Fig. 1. A schematic diagram of the electrochemical mechanism for the dissolution of pyrite. The oxidation (anodic) reaction and the reduction (cathodic) occur on the surface of the pyrite. Both anodic dissolution of pyrite and the cathodic reduction of ferric ions are functions of the potential across the mineral-solution interface. The thermodynamic driving force for the reaction is the difference between the cathodic equilibrium potential, $E_{e,\mathrm{Fe}}$, and the anodic equilibrium potential, $E_{e,\mathrm{FeS_2}}$. The overall reaction occurs at the mixed potential, E_m, at which the current due to the anodic processes is equal to the current due to the cathodic processes. The rate of dissolution is either the anodic or the cathodic current at the mixed potential.

the electrochemistry of the reaction has been reported. It is the aim of this paper to show that the kinetics of dissolution of pyrite are described by an electrochemical mechanism.

The dissolution of pyrite is an oxidation-reduction reaction since the pyrite is oxidized and the ferric ions and oxygen are reduced at the pyrite surface. The overall reaction can be written in terms of the half reactions for the oxidation of pyrite and the reduction of ferric ions. These half-reactions are the anodic oxidation of pyrite,

$$\mathrm{FeS_2} + 8\mathrm{H_2O} \rightarrow \mathrm{Fe^{2+}} + 2\mathrm{SO_4^{2-}} + 16\mathrm{H^+} + 14e^- \qquad (4)$$

and the cathodic reduction of ferric ions or dissolved oxygen,

$$\mathrm{Fe^{3+}} + e^- = \mathrm{Fe^{2+}}, \qquad (5)$$

$$\mathrm{O_2} + 4\mathrm{H^+} + 4e^- \rightarrow 2\mathrm{H_2O}. \qquad (6)$$

The observation that the oxygen in the sulphate comes from water is naturally explained by this electrochemical mechanism, shown in reaction (4). In spite of this clear indication that the electrochemistry of the process is of prime importance, there is no reported study of the electrochemistry of the oxidation of pyrite by ferric ions or by oxygen. [A distinction between reaction (4) and reaction (1) is necessary. Reaction (4) is referred to as the anodic dissolution of pyrite, whereas reactions (1) or (2) is referred to as the oxidative dissolution of pyrite.]

The rate of the reactions (4), (5), and (6) are exponentially dependent on the potential across the mineral-solution interface. They occur simultaneously on the entire surface of the dissolving pyrite at rates that satisfy the condition that the net production of electrons is zero. The potential at which this condition is met is called the mixed potential, or the corrosion potential. The electrochemical mechanism of dissolution is illustrated in Figure 1. Since the reactions (4), (5), and (6) occur independently, they can be studied separately, and rate expres-

sions for the individual half-reactions can be established. A kinetic expression for the rate of the overall reaction can be derived from the rate expressions for the half reactions using the condition that the net production of electrons is zero at the mixed potential (Nicol et al., 1975).

In addition, the overall reaction can be studied by measuring the mixed potential as a function of concentration. This potential is determined by measuring the potential difference between a corroding pyrite electrode and a reference electrode. Determination of the effects of concentration on the mixed potential is an independent verification of the rate equations that are determined from the analysis of the individual half-reactions and from empirical dissolution studies. Such measurements have not yet been reported for pyrite.

We report here the results of an electrochemical study of the mechanism of oxidation of pyrite under conditions similar to those found in bacterial leaching and in sites of acid mine drainage. We show that the kinetics is described by an electrochemical mechanism. We report experimental results for the individual half-reactions given by Eqns. (4), (5), and (6), and for the mixed potentials of the overall reaction. We derive rate expressions for the dissolution of pyrite, and we show that the reported literature data support these expressions.

2. EXPERIMENTAL METHODS

2.1. Materials and Apparatus

Cubic crystals of pyrite were obtained from Wards National Scientific Museum in Rochester, New York. The pyrite crystals originated from Logrono in Spain. The pyrite was determined to be an *n*-type semiconductor by thermoelectric measurement and by Hall effect measurement. The resistivity, measured by the four wire method (Shuey, 1975), was 75×10^{-3} Ω cm. Electrodes were constructed by contacting brass strips to the back of the pyrite with silver impregnated epoxy. Contact wires were soldered to the brass plates. The pyrite electrode was mounted in cold-setting araldite resin.

Analytical grade reagents were used in the experimental investigation. Sulphuric acid (98 wt.%) was used to obtain the desired pH or acid concentration in each experiment. Doubly distilled water was used to prepare all solutions. Ultra high purity nitrogen and oxygen was used.

The electrochemical kinetics was studied by steady-state voltammetry measurements using a standard three-electrode cell. The cell consisted of a pyrite working electrode, a platinum counter electrode, and a saturated calomel reference electrode. The calomel reference electrode was placed in a Luggin capillary. All potentials are referenced to the saturated calomel electrode (SCE). The three electrodes and the electrolyte solution were placed in a glass container fitted with a water jacket. Water from a constant water bath was pumped through the jacket. The container lid was fitted with an inlet for a gas sparger. The solution was agitated by a magnetic stirrer. A BAS CV-27 potentiostat was used to perform the voltammetry. The electrode potential and current were recorded by a data acquisition unit.

The kinetics of the dissolution of pyrite by ferric ions and dissolved oxygen was studied by mixed potential measurements. The mixed potential of pyrite was measured with respect to a calomel reference electrode using a BAS CV27 potentiostat or a Schlumberger Solartron 1286 potentiostat. A magnetic stirrer agitated the solution.

2.2. Electrochemical Experimental Procedures

The electrodes were prepared by polishing with 220, 600, and 1200 grade silicon carbide paper. The electrodes were then rinsed in distilled water and washed in acetone to remove any species that remained on the electrode surfaces after polishing. The electrodes were further washed and polished with a 5 micron alumina polishing compound. The polishing compound was removed by distilled water before the electrodes were placed in the cell.
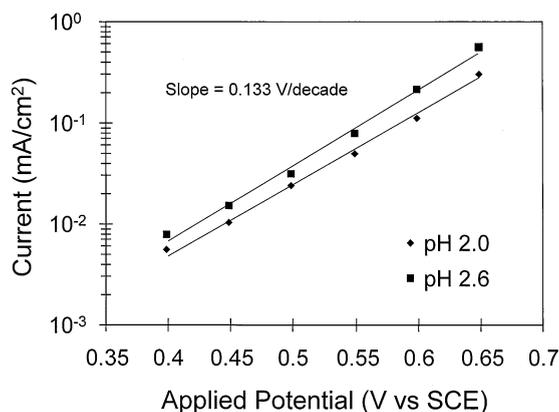
Fig. 2. The current due to the anodic dissolution of pyrite as a function of applied potential. Conditions: 308 K, N_2 sparged, 250 rpm.

Fig. 3. The effect pH on the anodic dissolution of pyrite at different applied potentials. Conditions: 308 K, N_2 sparged, 250 rpm.

The current–voltage behavior of the individual half-reactions was investigated using steady-state voltammetry. The procedure for the steady-state measurements consisted of preparing the acidic solution at the required concentrations, placing the solution and the electrodes in the cell, and de-aerating the solution by passing high purity nitrogen gas through the solution for at least 15 min prior to the electrochemical measurements. The pyrite working electrode, the platinum counter electrode, and the saturated calomel reference electrode were connected to the potentiostat. The applied potential was set at the desired value and held for at least 2 min. This measurement was increased in small increments over the desired potential range, and the current recorded at these potentials.

The procedure for the mixed potential measurements consisted of preparing an acidic solution and placing it in the cell. The solution was agitated by a magnetic stirrer. The pyrite electrode, the saturated calomel reference electrode, and platinum electrode were placed in solution. The mixed potential of the pyrite electrode with respect to the calomel reference electrode was measured by determining the potential difference between the two electrodes. The measurements were made at various concentrations of ferric and ferrous ions. The redox potential of the solution was also measured by determining the potential of the platinum electrode with respect to the calomel electrode.

2.3. Spectroscopy and Microscopy Techniques

Samples of the pyrite electrodes that had been treated by the application of an applied potential or that had been leached in solution in the mixed potential measurements were examined using Raman spectroscopy, X-ray photoelectron spectroscopy, and scanning electron microscopy.

The Raman spectra were obtained using a Jobin–Yvon T64000 spectrometer in spectrograph mode, together with an Olympus BH-40 microscope and LM Plan F1 × 20 lens. The samples for Raman spectroscopy were stored under a nitrogen atmosphere.

A Physical Electronics Quantum 2000 Scanning ESC microprobe spectrometer was used for the x-ray photoelectron spectroscopy (XPS). The spectra were recorded with monochromatized Al $K\alpha$ radiation of 1486.7 eV. A broad scan was made on each sample, and the $C1s$ peak was monitored for shifts in binding energy. The $S2p$ spectra were fitted with doublets of Gauss–Lorentzian distributions with a Shirley-type background.

A JEOL 840 scanning electron microscope was used to examine the pyrite surface.

3. RESULTS

3.1. The Anodic Oxidation of Pyrite

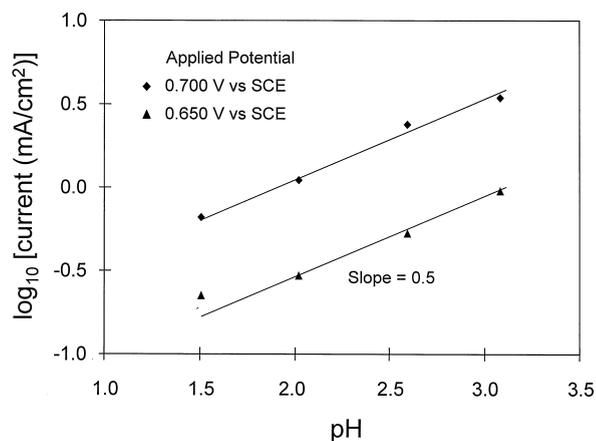The current-voltage characteristics of the anodic dissolution of pyrite, given by Eqn. (4), are presented in Figure 2. These results indicate that the current increased exponentially with applied potential, with a slope of 0.133 V/decade. The effects of temperature and pH on the anodic dissolution of pyrite were determined. The activation energy for the anodic dissolution of pyrite was 79.9 kJ/mol. The magnitude of the activation energy indicates that the anodic dissolution of pyrite is controlled by chemical kinetics. The effect of pH on the anodic dissolution of pyrite is shown in Figure 3. The order of reaction with respect to H^+ is -0.5, which is in agreement with the results of other researchers.

The anodic dissolution of pyrite results in the formation of sulphur and sulphate, and the sulphate yield is dependent on the potential (Bailey and Peters, 1976; Mishra and Osseo-Asare, 1988; Flatt and Woods, 1995). Since their data suggested a limit of about 50% for the sulphate yield at low potentials, Mishra and Osseo-Asare (1988) suggested a mechanism involving thiosulphate as the intermediate in the production of both sulphur and sulphate. These authors followed the mechanism proposed by Johnston and McAmish (1973) in which sulphur is formed from the decomposition of thiosulphate, while sulphate is formed from the electrochemical oxidation of thiosulphate. By stoichiometry, this mechanism means that at low potentials the sulphate yield will be 50%. However, Flatt and Woods (1995) presented data that suggest that there is no limit at lower potentials, since the sulphate yield at low potentials is below 50%. The data obtained in this study for the sulphate yield using the technique used by Bailey and Peters (1976), Mishra and Osseo-Asare (1988), and Flatt and Woods (1995) are shown in Fig. 4. The results agree with those of Flatt and Woods (1995). The implication of these results and those of Flatt and Woods (1995) is that sulphur is formed not only by the thiosulphate route.

The surfaces of the pyrite electrodes that had been anodically polarized at different applied potentials were examined by both Raman and XPS analysis. Both these techniques showed evidence for the presence of polysulphide material on the surface of pyrite, and the XPS analysis showed that the total amount of polysulphides on the surface increased with increasing applied potentials. Since the current increased exponentially with applied potential, as shown in Figure 2, the formation of this surface product does not limit the rate processes at the surface.
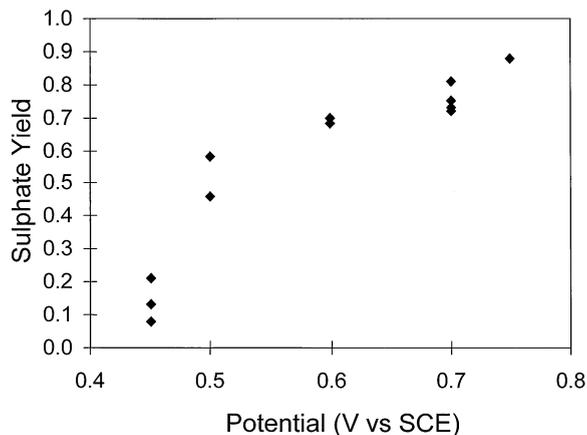
Fig. 4. The sulphate yield for the anodic dissolution of pyrite at various applied potentials. Conditions: 0.2 M H_2SO_4, 308 K, N_2 sparged, 250 rpm.

3.2. The Reduction of Ferric Ions and the Oxidation of Ferrous Ions on Pyrite

The current-voltage characteristics of the reduction of ferric ions on pyrite, given by reaction (5), were studied by steady-state voltammetry. In order to avoid the contribution of the anodic dissolution of pyrite to the total current, the reduction of ferric ions was studied at potentials that were cathodic to 0.55 V vs SCE. The results for the reduction of ferric ions are given in Figure 5 as a function of applied potential. At low values of the current, the current was exponentially dependent on the potential. As the current increases, the current becomes independent of the applied potential, indicating that the reaction becomes mass transfer controlled. The Tafel slopes for the reduction of ferric ions on pyrite ranged between 0.120 to 0.140 V/decade. The order of reaction with respect to ferric ions was 1.02 at 0.32 V, 0.97 at 0.36 V, and 1.07 at 0.44 V vs SCE. The effect of temperature was investigated, and the activation energy was found to be 45 kJ/mol. This value of activation energy suggests that the process is controlled by reaction, and not by diffusion.
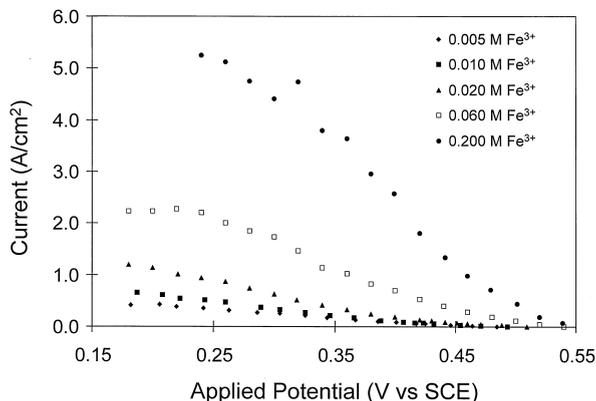

Fig. 5. The reduction of ferric ions on pyrite as a function of applied potential at various concentrations of ferric ions. Conditions: 0.2 M H_2SO_4, 0.1 M $FeSO_4$, 308 K, N_2 sparged, 250 rpm.
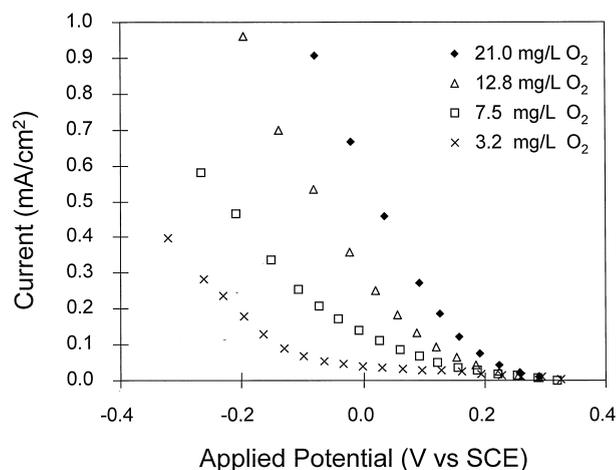

Fig. 6. The reduction of dissolved oxygen on pyrite as a function of applied potential at various concentrations of dissolved oxygen. Conditions: 0.2 M H_2SO_4, 308 K, N_2 sparged, 250 rpm.

The oxidation of ferrous ions on pyrite is difficult to measure independently due to the contribution of the anodic dissolution of the pyrite to the measured current. However, this work indicated that the reaction is first order in ferrous ions, and has a Tafel slope that is similar in value to that of the oxidation of ferrous ions on pyrite, that is, between 0.120 and 0.140 V/decade.

3.3. The Reduction of Dissolved Oxygen on Pyrite

The current–voltage characteristics of the reduction of oxygen on pyrite, given by reaction (6), were studied by steady-state voltammetry. The effect of the applied potential on the rate of reduction of dissolved oxygen on pyrite at different concentrations of oxygen is shown in Figure 6. The reaction is controlled by kinetic considerations at low currents, and by mass transfer processes at high currents. Since the equilibrium potential of the oxygen–water redox couple is approximately 0.99 V vs SCE at 0.2 M H_2SO_4, it is apparent that the reduction of oxygen is characterized by slow kinetics. The Tafel slope for the reduction of dissolved oxygen on pyrite between 0.3 V vs SCE and 0.15 V vs SCE was 0.115 V/decade at a dissolved oxygen concentration of 21 mg/L. The value of 0.115 V/decade for the Tafel slope compares favorably with the value of 0.125 V/decade reported by Biegler, Rand, and Woods (1975) for the reduction of oxygen on pyrite at saturated oxygen concentrations.

The reaction order for the reduction of dissolved oxygen on pyrite was 1.09 at 0.15 V and 1.05 at 0.175 V vs SCE. The reduction of oxygen was weakly dependent on the pH, as shown in Figure 7. The order of reaction with respect to H^+ was 0.14.

3.4. The Mixed Potential of Pyrite as a Function of Fe(II) and Fe(III) Concentration

The effect of the concentration of ferric ions on the mixed potential of pyrite is shown in Figure 8. The mixed potential of pyrite increases logarithmically with the concentration of ferric
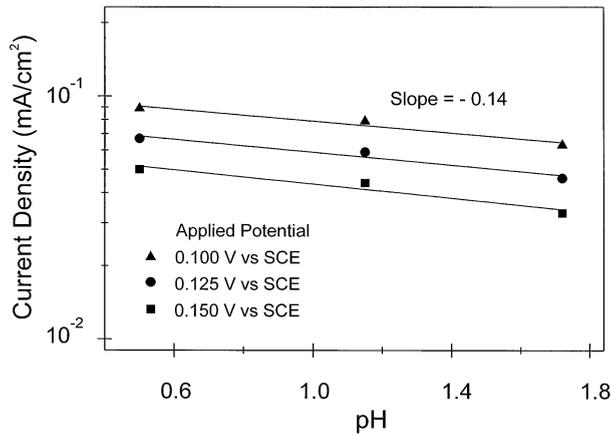
Fig. 7. The effect of pH on the reduction of oxygen at various applied potentials. Conditions: 308 K, N_2 sparged, 250 rpm.

Fig. 9. Mixed potential of pyrite and redox potential as a function of concentration of ferrous ions. Conditions: 1 M Na_2SO_4, 0.025 M Fe^{3+}, 298 K, N_2 sparged, 250 rpm.

ions. At low concentrations of ferrous ions, the mixed potential of pyrite is less than the redox potential of the solution. At higher concentrations of ferrous ions, the mixed potential and the redox potential have similar values. The slope of the line in Fig. 8 is 0.056 V/decade. It is important to note that the mixed potential is not equal to the redox potential.

The effect of the concentration of ferrous ions on the mixed potential of pyrite is shown in Figures 9 and 10. These results show that at low concentrations of ferrous ions, the mixed potential is independent of the concentration. The mixed potential is logarithmically dependent on the concentration of ferrous ions with a slope of -0.056 V/dec. The dependence of the mixed potential the pH of the solution is shown in Figure 11. The slope of the mixed potential with respect to pH is -0.029 V/pH unit at low concentrations of ferrous ions. The mixed potential was independent of the conditions of agitation of the solution.

Some previous work has suggested that the rate of dissolution is dependent on the total concentration of iron in solution (Garrels and Thompson, 1960; Mathews and Robins, 1972; Lowson, 1982). The mixed potential of pyrite was measured as
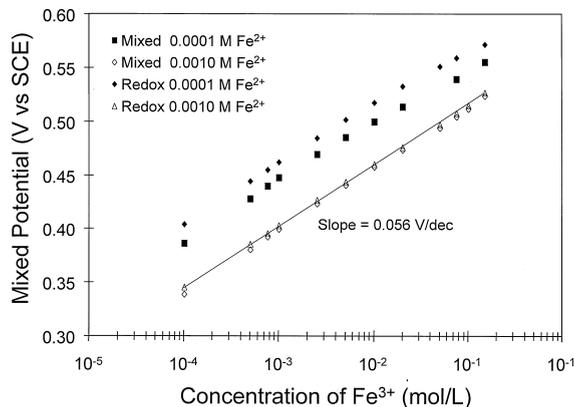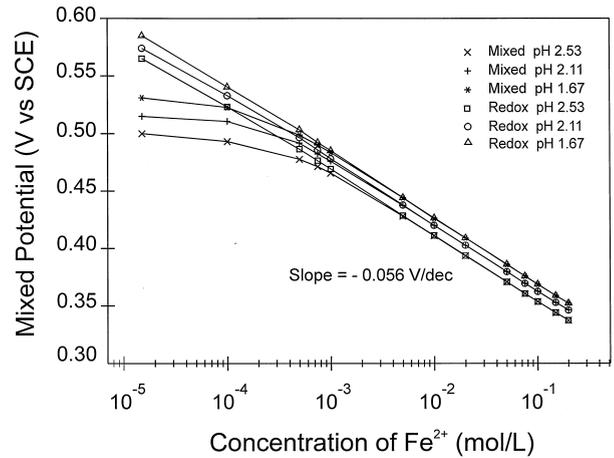
a function of the total concentration of dissolved iron at a constant ratio of ferric ions to ferrous ions. The results, shown in Figure 12, indicate that the mixed potential is constant as the total concentration of iron increases at a constant ratio of ferric to ferrous ions.

Pyrite samples were leached for 14 days in ferric sulphate solutions containing 9 g/L total iron at a pH of 1.6, a redox potential of 0.65 V (vs SCE) and at 35°C. The Raman spectra for these samples indicated strong pyrite peaks at 342 and 378 cm^{-1}, and a weak and broad peak between 430 and 470 cm^{-1}. This last peak was assigned to a range of polysulphides (Buckley and Woods, 1987; Janz et al., 1976a, 1976b; Li and Wadsworth, 1993; Mycroft et al., 1990). This last peak increased slightly with increased leaching time.

It has often been suggested that the product species, such as polysulphides, form on the pyrite surface and inhibit the rate of reaction. In order to test whether the pyrite surface was altered by the accumulation of these reaction products, the mixed
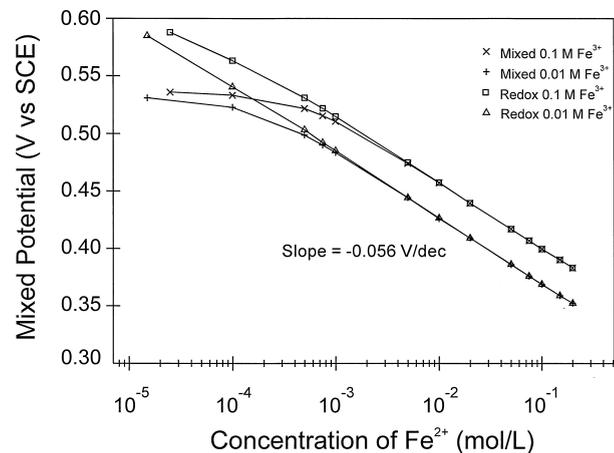

Fig. 8. Mixed potential of pyrite as a function of the concentration of ferric ions. Conditions: 0.037 M H_2SO_4, 1 M Na_2SO_4, 298 K, N_2 sparged, 250 rpm.

Fig. 10. Mixed potential of pyrite and redox potential as a function of ferrous ions. Conditions: pH 1.67, 1 M Na_2SO_4, 298 K, N_2 sparged, 250 rpm.
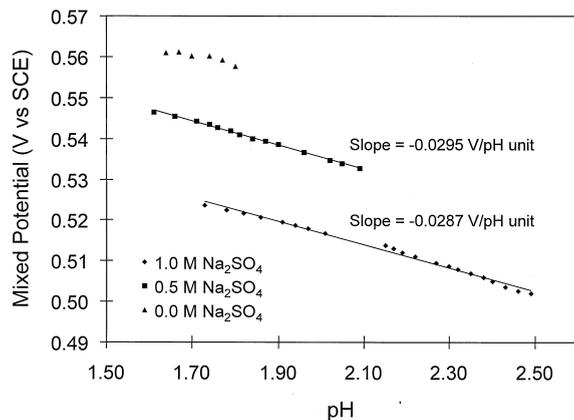
Fig. 11. The effect of pH on the mixed potential. Conditions: 1 M Na$_2$SO$_4$, 0.025 M Fe^{3+}, 0.0001 M Fe^{2+}, 298 K, N$_2$ sparged, 250 rpm.

potentials of the pyrite that had been leached for 7 and 14 days in a flow-through reactor (Holmes et al., 1999) were determined. The leaching was conducted in a solution of ferric sulphate containing 9 g/L total iron at a pH of 1.6 and at 35°C. The redox potential of this solution was 0.65 V vs SCE. The results for these mixed potentials after leaching for 7 and 14 days are compared in Figure 13 with those of polished pyrite. The results shown in Figure 13 indicate that there is no change in the mixed potential with leaching time. These results indicate that the formation and accumulation of surface products does not affect the electrochemical characteristics of the surface. In addition, it is shown later in this paper that the rate of reaction is controlled by the electrochemical steps. Therefore, the accumulation of surface products, such as polysulphides, does not affect the rate of dissolution in ferric sulphate solutions.

The surfaces of pyrite that had been either anodically polarized at different applied potentials or exposed to solutions of ferric sulphate both showed similar corrosion patterns when viewed by electron scanning microscopy. More polysulphide material was detected by XPS and Raman spectroscopy on the surface of anodically polarized pyrite than on the surface of pyrite exposed to ferric sulphate solutions for extended periods.
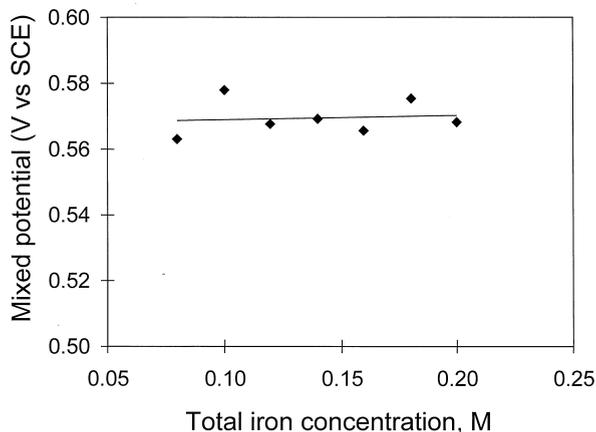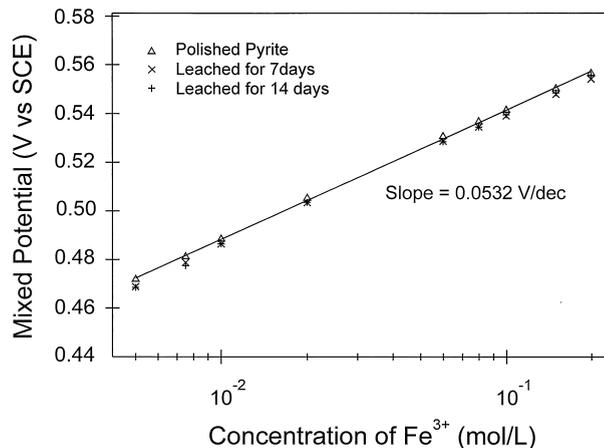
Fig. 13. The effect of leaching the pyrite at a redox potential of 0.65 V (vs SCE), pH 1.6, and 308 K for 7 and 14 days on the mixed potential. Conditions of mixed potential measurement: pH 1.45, 0.001 M Fe^{2+}, 308 K, 250 rpm.

3.5. Mixed Potential of Pyrite in the Presence of Ferric Ions and Dissolved Oxygen

The mixed potential of pyrite in the presence of both ferric ions and dissolved oxygen is shown in Figure 14. The mixed potential of pyrite is unaffected by the presence of oxygen at low concentrations of dissolved oxygen. However, at a dissolved oxygen concentration of 21 ppm, the mixed potential of pyrite at various ferric concentrations is greater than the mixed potential of pyrite in the absence of dissolved oxygen.

The mixed potentials of pyrite in oxygenated solutions oxygen were close to the rest potential of pyrite. This result suggests that kinetics of reduction of oxygen is very slow, and that the rate of dissolution of pyrite with oxygen is much slower than that with ferric ions.

Fig. 12. The effect of changes in the total concentration of iron at a constant ratio of ferric to ferrous ions of 2000. Conditions: 0.15 M H$_2$SO$_4$, 308 K, N$_2$ sparged, 250 rpm.
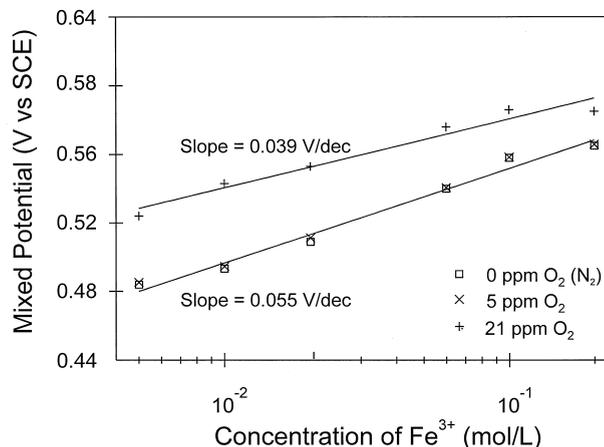
Fig. 14. The effect of the concentration of ferric ions on the mixed of pyrite at various concentrations of dissolved oxygen. Conditions: pH 1.45, 0.001 M Fe^{2+}, 308 K, 250 rpm.

4. DEVELOPMENT OF KINETIC EXPRESSIONS FOR THE MIXED POTENTIAL AND THE RATE OF LEACHING OF PYRITE

The dissolution of pyrite occurs as a combination of the anodic dissolution of pyrite and the reduction of ferric ions or oxygen on the surface as given by Eqns. (4)–(6). The mixed potential is dependent on the rates of these half-reactions. In other words, the mixed potential of the corroding pyrite is a direct measure of the electrochemical state of the pyrite surface during dissolution. In this section, expressions for the mixed potential and the rate of dissolution of pyrite are developed, and these rate expressions are compared with the measurements of the mixed potential and with the published rate expressions.

4.1. The Anodic Dissolution of Pyrite

The anodic dissolution of pyrite, given by Eqn. (1), has been studied in detail (Bailey and Peters, 1976; Ahlberg and Broo, 1997; Biegler and Swift, 1979; Peters and Majima, 1968; Meyer, 1979; Mishra and Osseo-Asare, 1988; Kelsall et al., 1996). The results presented in Figures 2 and 3 indicate that the current density due to dissolution of the pyrite, i_{FeS_2}, is dependent on the potential, E, and the concentration of H^+, $[H^+]$, and is given by

$$i_{FeS_2} = k_{FeS_2}[H^+]^{-1/2} \exp\left(\frac{\alpha_{FeS_2}FE}{RT}\right), \qquad (7)$$

where k_{FeS_2} is the rate constant, α_{FeS_2} is the transfer coefficient, F is the Faraday constant, R is the gas constant, and T is the temperature. The Tafel slope is given by $2.303RT/(\alpha_{FeS_2}F)$; therefore a Tafel slope of 0.133 V/decade yields a value of 0.46 for α_{FeS_2}. These results are in agreement with those in the literature.

4.2. The Oxidation and Reduction of Dissolved Iron on Pyrite

The measured results at potentials cathodic of the rest potential are described by both chemical kinetics and mass transfer. However, in the region of potential above 0.40 V vs SCE the reduction of ferric ions is controlled by kinetic considerations alone. Because the mixed potentials are above 0.40 V vs SCE, the region above 0.40 V vs SCE is the region of interest. The current density due to oxidation and reduction of dissolved iron at the pyrite surface, i_{Fe}, given by Eq. (5), is described by

$$i_{Fe} = k_{Fe^{2+}}[Fe^{2+}] \exp\left(\frac{\alpha_{Fe}FE}{RT}\right)$$
$$- k_{Fe^{3+}}[Fe^{3+}] \exp\left(\frac{-(1-\alpha_{Fe})FE}{RT}\right), \quad (8)$$

where $[Fe^{3+}]$ is the concentration of ferric ions, $[Fe^{2+}]$ is the concentration of ferrous ions, $k_{Fe^{2+}}$ is the ferrous oxidation rate constant, $k_{Fe^{3+}}$ is the ferric reduction rate constant and is α_{Fe} is transfer coefficient for this reaction. The measured Tafel slope, given by $2.303RT/(\alpha_{Fe}F)$ was close to 0.120 V/decade, which yields a value of 0.51 for α_{Fe}.

4.3. The Reduction of Oxygen on Pyrite

The reduction of oxygen is described by chemical kinetics and mass transfer. In the region of potentials in which dissolution occurs, the reduction of oxygen at pyrite is described by reaction kinetics. The reaction was found to be weakly dependent on the pH. The current density due to the reduction of oxygen at the pyrite surface, i_{O_2}, is described by

$$i_{O_2} = -k_{O_2}[O_2][H^+]^{0.14} \exp\left(\frac{-(1-\alpha_{O_2})FE}{RT}\right), \qquad (9)$$

where $[O_2]$ is the concentration of dissolved oxygen, and α_{O_2} is the transfer coefficient for this reaction. The measured value of the Tafel slope was 0.115 V/decade, which gives a value of 0.53 for α_{O_2}.

4.4. Development of an Electrochemical Model for the Mixed Potential of Pyrite

During the dissolution of pyrite, the oxidation and reduction reactions (4), (5), and (6) occur simultaneously on the surface of the pyrite. The rate of these reactions and the potential at the surface is established to satisfy the condition that the net rate of production of electrons is zero. This is because there is no net current or accumulation of charge during dissolution. In addition, the anodic and cathodic half-reactions occur over the entire surface of the pyrite.

Since the net production of electrons is zero, and the surface area for both half-reactions is the same, it is clear that the following condition holds at the mixed potential, E_m:

$$i_{FeS_2} = -i_{Fe}. \qquad (10)$$

Substitution of Eqns. (7) and (8) into Eqn. (10) gives the following implicit expression for the mixed potential of a corroding pyrite surface, E_m:

$$k_{FeS_2}[H^+]^{-1/2} \exp\left(\frac{\alpha_{FeS_2}FE_m}{RT}\right) = -k_{Fe^{2+}}[Fe^{2+}] \exp\left(\frac{\alpha_{Fe}FE_m}{RT}\right)$$
$$+ k_{Fe^{3+}}[Fe^{3+}] \exp\left(\frac{-(1-\alpha_{Fe})FE_m}{RT}\right). \quad (11)$$

If the approximation is made that $\alpha_{FeS_2} \approx \alpha_{Fe} = 1/2$, this expression can be simplified to obtain the following explicit expression for the mixed potential:

$$E_m = \frac{RT}{F} \ln\left(\frac{k_{Fe^{3+}}[Fe^{3+}]}{k_{FeS_2}[H^+]^{-1/2} + k_{Fe^{2+}}[Fe^{2+}]}\right). \qquad (12)$$

The slope of the mixed potential with respect to ferric ions is $2.303RT/F$ V/decade = 0.059 V/decade. The theoretical value is in close agreement with the measured value of 0.056 V/decade that was determined from the results shown in Figure 8.

It is clear from Eqn. (12) that there are two limiting forms the mixed potential of pyrite in solutions of ferrous and ferric ions. If $k_{FeS_2}[H^+]^{-1/2} \gg k_{Fe^{2+}}[Fe^{2+}]$, then the mixed potential and the rate of leaching are independent of the concentration of ferrous ions. This condition is met at relatively low concentrations of ferrous ions and high values of the pH. The results presented in Figs. 9 and 10 show that at concentrations of ferrous ions below 0.0001 M, the mixed potential is independent of the concentration of ferrous ions.

As the concentration of ferrous ions is increased, the condition reverses so that $k_{FeS_2}[H^+]^{-1/2} \ll k_{Fe^{2+}}[Fe^{2+}]$, and the mixed potential is dependent on the concentration of ferrous ions. Under these conditions, the slope of the mixed potential against the logarithm of the concentration of ferrous ions should be $2.303RT/F = 0.059$ V/decade. The slope of results presented in Figs. 9 and 10 is 0.056 V/decade, which agrees very closely with the theory developed here.

When $k_{FeS_2}[H^+]^{-1/2} \gg k_{Fe^{2+}}[Fe^{2+}]$, the mixed potential is dependent on the pH of the solution. The slope of the mixed potential against the pH is $2.303RT/2F = -0.0305$ V/pH unit. The results are shown in Figure 11 indicate that the measured slope is -0.0287 and -0.0295 V/decade. These values are in very close agreement with the value predicted from the mixed potential theory.

If $k_{FeS_2}[H^+]^{-1/2} \ll k_{Fe^{2+}}[Fe^{2+}]$, then the mixed potential is determined by the concentrations of the ferrous and ferric ions in solution. In this case the value of the mixed potential is close to that of the redox potential. The Nernst equation for the redox potential is given by

$$E_{redox} = E^0_{redox} \frac{RT}{F} \ln\left(\frac{a(Fe^{3+})}{a(Fe^{2+})}\right),\tag{13}$$

where $a(Fe^{3+})$ and $a(Fe^{2+})$ are the activities of the ferric and ferrous ions in solution. Although the values of the mixed potential and the redox potential are close when $k_{FeS_2}[H^+]^{-1/2} \ll k_{Fe^{2+}}[Fe^{2+}]$, it must be emphasized that mixed potential and the redox potential are not the same. The mixed potential, given by Eqn. (12) is a kinetic measurement, while the redox potential, given by Eqn. (13), is a thermodynamic measurement. The term $k_{FeS_2}[H^+]^{-1/2}$, which arises from the anodic half-reaction of pyrite, appears in the denominator of Eqn. (12), but does not appear in the Nernst equation for the redox potential. The difference between the two potentials is largest at the conditions found in acid drainage and bacterial leaching where the concentration of ferrous ions is low. This is clearly shown in Figures 9 and 10. The treatment of the two as the same, mainly as an implicit assumption in previous work, is erroneous.

The mixed potential is dependent on the concentrations of ferric and ferrous ions in solution. The mixed potential is not affected by the total concentration of iron in solution when the ratio of ferric and ferrous ions is constant, which is in agreement with the results obtained.

The expression for the mixed potential derived from the measurements of the individual half reactions is in close agreement with the measurements of the mixed potential. Therefore, it is clear that the electrochemical theory describes the mixed potential of the pyrite surface during dissolution in the presence of dissolved iron. The mixed potential measurements are constant over a period of 14 days, indicating that there is no chemical change in the condition of the surface that affects the dissolution processes at extended periods. This means that the dissolution of pyrite by ferric ions, given by reaction (1), is governed only by the electrochemistry occurring at the pyrite surface.

4.5. Mixed Potential of Pyrite in the Presence of Oxygen and Dissolved Iron

In the presence of ferric ions and oxygen in solution, the condition that the net production of electrons is zero gives the following:

$$i_{FeS_2} = -i_{Fe} - i_{O_2}.\tag{14}$$

Substituting the expressions for i_{FeS_2}, i_{Fe}, and i_{O_2}, given by Eqns. (7), (8), and (9), into Eqn. (14), and making the assumption that $\alpha_{FeS_2} \approx \alpha_{Fe} \approx \alpha_{O_2} = 1/2$, the following expression is obtained for the mixed potential of pyrite in the presence of both ferric ions and dissolved oxygen:

$$E_m = \frac{RT}{F} \ln\left(\frac{k_{Fe^{3+}}[Fe^{3+}] + k_{O_2}[O_2][H^+]^{0.14}}{k_{FeS_2}[H^+]^{-1/2} + k_{Fe^{2+}}[Fe^{2+}]}\right).\tag{15}$$

When $k_{Fe^{3+}}[Fe^{3+}] \gg k_{O_2}[O_2][H^+]^{0.14}$, for example, at low concentrations of dissolved oxygen, the concentration of oxygen does not affect the mixed potential. As the concentration of dissolved oxygen increases, the mixed potential is affected. Under the condition where both the concentration of ferric ions and dissolved oxygen affect the mixed potential, as shown in Figure 14.

4.6. Development of Rate Expressions for the Dissolution of Pyrite

An expression for the rate of leaching, r_{FeS_2}, may be obtained by noting that the rate and the current density are related by stoichiometry, expressed by Faraday's equation:

$$r_{FeS_2} = \frac{i_{FeS_2}}{14F}.\tag{16}$$

Combining Eqns. (7), (12), and (15) yields an expression for the rate of leaching of pyrite:

$$r_{FeS_2} = \frac{k_{FeS_2}[H^+]^{-1/2}}{14F}\left(\frac{k_{Fe^{3+}}[Fe^{3+}]}{k_{FeS_2}[H^+]^{-1/2} + k_{Fe^{2+}}[Fe^{2+}]}\right)^{1/2}.\tag{17}$$

Equation (17) indicates that the order of reaction with respect to Fe^{3+} is 0.5. If $k_{FeS_2}[H^+]^{-1/2} \gg k_{Fe^{2+}}[Fe^{2+}]$, then order of reaction with respect to Fe^{2+} is zero, and that with respect to H^+ is -0.25. If $k_{FeS_2}[H^+]^{-1/2} \ll k_{Fe^{2+}}[Fe^{2+}]$, then the reaction order with respect to Fe^{2+} is -0.5, and with respect to H^+ is -0.5. Therefore, there is a range of reaction orders with respect to Fe^{2+} and H^+ expected from the electrochemical model derived here.

In the presence of oxygen, the rate of leaching of pyrite is obtained by combining Eqns. (7), (15), and (16). This expression is given by

$$r_{FeS_2} = \frac{k_{FeS_2}[H^+]^{-1/2}}{14F}\left(\frac{k_{Fe^{3+}}[Fe^{3+}] + k_{O_2}[O_2][H^+]^{0.14}}{k_{FeS_2}[H^+]^{-1/2} + k_{Fe^{2+}}[Fe^{2+}]}\right)^{1/2}.\tag{18}$$

In the absence of dissolved iron in the leaching solution, the rate expression is given by

$$r_{FeS_2} = \frac{k_{FeS_2}[H^+]^{-0.18}}{14F}\left(\frac{k_{O_2}[O_2]}{k_{FeS_2}}\right)^{1/2}.\tag{19}$$

Thus, in the absence of dissolved iron, the orders of reaction

Table 1. Rate expressions for the dissolution of pyrite in solutions containing dissolved iron.

Reference	Rate expression
Garrels and Thompson (1960)	$r_{FeS_2} = \dfrac{k[Fe^{3+}]}{\sum[Fe]}$
Smith and Shumate (1970)	$r_{FeS_2} = \dfrac{k_2[Fe^{3+}]^{0.5} - k_2[Fe^{2+}]^{0.5}}{1 + k_3[Fe^{3+}]^{0.5} + k_4[Fe^{2+}]^{0.5}}$
Mathews and Robins (1972)	$r_{FeS_2} = \dfrac{k[Fe^{3+}]}{\sum[Fe][H^+]^{0.44}}$
Lowson (1982)	$r_{FeS_2} = \dfrac{k[Fe^{3+}][Fe^{2+}]}{\sum[Fe]}$
McKibben and Barnes (1986)	$r_{FeS_2} = \dfrac{k[Fe^{3+}]^{0.58}}{[H^+]^{0.5}}$
Williamson and Rimstidt (1994)	$r_{FeS_2} = \dfrac{k[Fe^{3+}]^{0.3}}{[H^+]^{0.32}[Fe^{2+}]^{0.47}}$
Present work—electrochemical measurement and theory	$r_{FeS_2} = k[H^+]^{-0.5}\left(\dfrac{k_{Fe^{3+}}[Fe^{3+}]}{k_{FeS_2}[H^+]^{-0.5} + k_{Fe^{2+}}[Fe^{2+}]}\right)^{0.5}$

predicted from the electrochemical measurements are 0.5 with respect to O_2 and -0.18 with respect to H^+.

4.7. Comparison of the Electrochemical Rate Equations with the Empirical Rate Equations

The rate equations that have been presented by other researchers for the oxidation of pyrite by ferric ions are presented in Table 1. Garrels and Thompson (1960) proposed that the rate of oxidation of pyrite is inversely proportional to the total iron concentration. This rate equation means that in the absence of ferrous ions the rate of the oxidative dissolution of pyrite is independent of the concentration of ferric ions. This is clearly erroneous since the dissolution process requires an oxidant. The rate equation proposed by Lowson (1982) also relates the rate of the oxidative dissolution of pyrite by ferric ions to the inverse of the total iron concentration. The results presented here show that the mixed potential is independent of the total iron concentration at a constant ratio of ferric ions to ferrous ions. By the electrochemical arguments given above, this means that the rate is not a function of the total concentration of iron in solution at a constant ratio of ferric ions to ferrous ions. Wiersma and Rimstidt (1984) assumed that the rate of the oxidative dissolution of pyrite by ferric ions was a first order process in ferric ions only. McKibben and Barnes (1986) observed that the rate of the oxidative dissolution of pyrite was dependent on the concentration of ferric ions and protons, with reactions orders of 0.58 and -0.5, respectively. Their results are described by the one limiting form of the rate expression developed here, that is, when $k_{FeS_2}[H^+]^{-1/2} \ll k_{Fe^{2+}}[Fe^{2+}]$, the rate expression obtained in this study has orders of reaction that are the same as those obtained by McKibben and Barnes (1986).

Williamson and Rimstidt (1994) used nonlinear regression to fit an equation to the data collected from their work and other researchers. They obtained a reaction order with respect to ferric ions of 0.3, which is lower than the value of 0.58 found by McKibben and Barnes (1986). The reaction order may be

smaller than that of McKibben and Barnes (1986) because Williamson and Rimstidt (1994) used data from a number of sources to develop their rate expression. This data included that from Smith and Shumate (1970) for the dissolution of pyrite in acidic conditions. The reaction order with respect to H^+ reported by Williamson and Rimstidt (1994) lies between the order of reaction obtained from two limiting forms of Eqn. (16), that is, between -0.5 and -0.25. When the condition that $k_{FeS_2}[H^+]^{-1/2} \ll k_{Fe^{2+}}[Fe^{2+}]$ holds, the Eqn. (15) has the same order of reaction as that found by Williamson and Rimstidt (1994).

The empirical rate equations that have been proposed for the oxidative dissolution of pyrite by dissolved oxygen are given in Table 2. Mathews and Robins (1972) found that the rate of reaction had an order of reaction of 0.81 with respect to the concentration of dissolved oxygen. They found that the rate was independent of the pH. McKibben and Barnes (1986) observed that the rate of the oxidative dissolution of pyrite by dissolved oxygen had a half order dependence on the dissolved oxygen concentration and was independent of the proton concentration. Williamson and Rimstidt (1994) also found a half order dependence of the rate on the concentration of dissolved

Table 2. Rate expressions for the dissolution of pyrite in solutions containing dissolved oxygen.

Reference	Rate expression
Mathews and Robins (1974)	$r_{FeS_2} = k[O_2]^{0.81}$
Bailey and Peters (1976)	$r_{FeS_2} = k_1\left(\dfrac{[O_2]}{k_2 + [O_2]}\right)^{0.5}$
McKibben and Barnes (1986)	$r_{FeS_2} = k[O_2]^{0.5}$
Williamson and Rimstidt (1994)	$r_{FeS_2} = \dfrac{k[O_2]^{0.5}}{[H^+]^{0.11}}$
Present work–electrochemical measurement and theory	$r_{FeS_2} = k[H^+]^{-0.18}[O_2]^{0.5}$

oxygen. In addition, they found a weak dependence of the rate on the pH. This data included that from Smith and Shumate (1970) and Moses and Herman (1991) for the dissolution of pyrite in acidic and basic conditions, respectively.

The electrochemical measurements and methods used here predict that the rate of reaction is half-order in oxygen and weakly dependent on pH. This electrochemical rate equation derived here is close to that obtained by Williamson and Rimstidt (1994).

5. DISCUSSION

None of the previous work has been able to successfully explain the half-order kinetics with respect to the ferric ions or oxygen that has been reported in the literature for the dissolution of pyrite. The electrochemical mechanism successfully predicts the half-order kinetics. In addition, this mechanism successfully explains the effect of the ferrous ions and pH. Thus, it is concluded that the kinetics of dissolution of pyrite in solutions containing ferric ions and dissolved oxygen is described by the electrochemical model derived here, and that the rate-determining step is the transfer of charge at the mineral-solution interface. The range of conditions over which this holds is wide, since the work of Bailey and Peters (1976) was done at temperatures of 110°C.

The results showed that even after leaching the pyrite for 14 days, the mixed potential was the same as that of polished pyrite. Since the mixed potential and the rate of dissolution are uniquely correlated, this means that factors affecting the rate of dissolution of pyrite do not change over time. The surface analysis indicated the presence of small quantities of polysulphides, in agreement with previous work (Kelsall et al., 1996). However, this work has shown that the kinetics of dissolution cannot be explained on the basis of observations of the surface products.

The dissolution of pyrite in most cases produces both sulphur and sulphate as the final products. Moses et al. (1987) observed sulphate as the only soluble reaction product during pyrite oxidation by ferric ions and dissolved oxygen at pH 2.2 Sulphate was proposed to form by the progressive oxidation of intermediate sulphur-oxy species such as thiosulphate and polythionates. McKibben and Barnes (1986) observed small amounts of polythionates during pyrite oxidation by dissolved oxygen at pH 3.6.

The sulphate yield for the anodic dissolution reaction tends to zero at low potentials. This result does not support the hypothesis that thiosulphate is the primary intermediate for the production of sulphur. The sulphate yields determined for the anodic dissolution of pyrite indicate that sulphur and sulphate formed by independent electrochemical routes. The sulphate yield is not fixed, but a function of electrode potential. This means that the sulphate yield will change as the mixed potential of the pyrite changes.

Much research has been performed on the bacterial leaching of pyrite. Bacteria affect the rate of formation of acid-mine drainage, and influence the iron and sulphur cycles in nature. The implication of the present work is that if the bacteria increase the rate of leaching above that achieved by chemical means at the same conditions in solution, they must affect the electrochemistry of the process. The bacteria may achieve this

by secreting an oxidant that has greater oxidizing capacity than ferric ions, or by altering the local environment at the surface of pyrite. Both of these effects will affect the mixed potential. Holmes, Fowler, and Crundwell (1999) found that the presence of bacteria on the pyrite surface lowered the mixed potential at low concentrations of ferrous ions. In addition, Fowler, Holmes, and Crundwell (1999) found that the bacteria increase the rate of dissolution above that achieved chemically at the same solution conditions. The analysis leading to Eqns. (12) and (17) shows that the only explanation for an increase in rate and a decrease in mixed potential at low concentrations of ferrous ions is that the bacteria increase the pH at the mineral surface.

Pyrite is a semiconductor, and since the kinetics of dissolution is described by an electrochemical mechanism, the semiconducting properties influence the kinetics of dissolution (Crundwell, 1988a, 1988b; Doyle and Mishra, 1996). Illumination of the pyrite surface increases the anodic dissolution of n-type pyrite (Jaegermann and Tributsch, 1984; Mishra and Osseo-Asare, 1988; Schubert and Tributsch, 1990; Chen et al., 1991; Salvador et al., 1991; Brouold et al., 1994; Mishra and Osseo-Asare, 1992). This suggests that the light generated holes react at the surface, and indicates that the semiconductor properties influence the kinetics. However, the value of the Tafel slope is not that expected for a semiconductor, and Springer (1970) found that the Tafel slope of n- and p-type pyrite is the same in the anodic potential region. Bryson (1999) proposed that the dissolution reaction is influence by the presence of a surface state. He derived a model in which it is shown that the surface state influences the dissolution process so that p- and n-type pyrite have the same Tafel slope, and illumination increases the rate of anodic dissolution.

The band-energy model is often used to describe processes at the semiconductor-solution interface. The mechanism for the oxidative dissolution of pyrite proposed in this work is illustrated in terms of the band-energy diagram shown in Figure 15. The band-energy diagram is a plot of electronic energy against distance in the semiconductor side of the interface, and probably density on the solution side of the interface. The energy levels of the solution species are distributed with energy due to the thermal fluctuations of the bonds between the solution species and the water. At equilibrium, the Fermi levels of both the solid and the solution are equal. During oxidative dissolution, the effect of the ferric ions in solution is to displace the Fermi levels in the solid and the solution by an amount that represents the mixed potential, and which results in the net transport of electrons from the solid via the surface state to the ferric ions in solution, resulting in the dissolution of the solid and the reduction of the ferric ions. The rate at which these processes occur is described by the mixed potential model derived in this paper. Therefore, the electrochemical mechanism proposed here accounts for all the observations concerning the dissolution of pyrite by ferric ions (or oxygen), and the observations concerning the anodic dissolution of pyrite.

6. CONCLUSIONS

Electrochemical techniques and theory were used to study the kinetics of the half reactions involved in the oxidation of pyrite. Several conclusions can be drawn from this research:
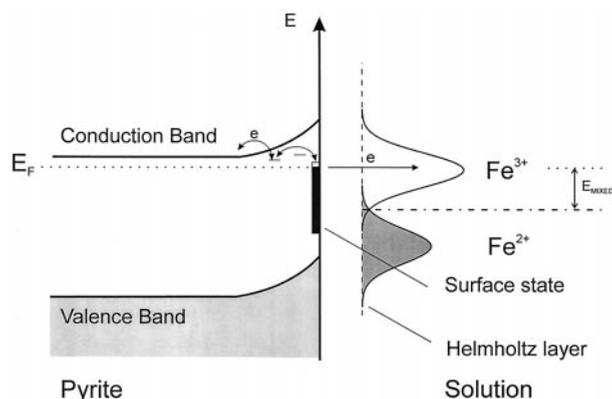
Fig. 15. The energy-band diagram for the dissolution of pyrite in ferric sulphate solutions. The diagram shows the solid and solution energy levels at the pyrite-solution interface. The solid is represented by a plot of energy versus distance, while the solution is represented as a plot of energy versus density of levels at that energy level. The electronic structure of the pyrite surface is that of a semiconductor with a depletion layer and a surface state. The Fermi level of the solid is represented by E_F. The density of states of ions in solution is described by the fluctuating energy level model (Crundwell, 1988a; 1988b). As electrons are removed from the surface state by the ferric ions, dissolution of the surface occurs. The rate of dissolution is governed by the mixed potential condition, illustrated in Figure 1.

(1) The observation by Reedy et al. (1991), Taylor et al. (1984a, 1984b), and Bailey and Peters (1976) that the oxygen in the sulphate product originates from water is a direct consequence of the electrochemical mechanism. Thus, the oxidation of pyrite by ferric ions and dissolved oxygen is an electrochemical process.

(2) The anodic dissolution of pyrite and the reduction of ferric ions and oxygen were all studied separately. These half-reactions are governed by charge transfer processes in the region of potentials in which pyrite dissolves.

(3) An electrochemical (or mixed potential) model was derived using the results obtained from the study of the individual half reactions. The oxidation and reduction reactions occur over the entire surface of the pyrite subject to the condition that the net production of electrons must be zero. The mixed potential model derived here successfully describes the measured mixed potentials, and is consistent with the reported rate expressions for oxidative dissolution of pyrite by both ferric ions and oxygen.

(4) The mixed potential was used as a measurement of the kinetics of the overall reaction. The measurements of the mixed potential were made as a function of the concentration of ferric and ferrous ions and of pH. The electrochemical mechanism describes these measurements. It is important to realize that mixed potential is not the same as the redox potential.

(5) The mixed potential does not change over a 14-day period of leaching. This indicates that no products accumulate on the surface that influence the kinetics of dissolution. XPS and Raman spectroscopy was used to examine the surface. A small amount of polysulphide material was detected after 14 days of leaching in a ferric sulphate solution, but the observation that the mixed potential is unaffected means that the presence of polysulphide material does not influence the kinetics of dissolution.

(6) The sulphate yields obtained from the anodic dissolution of pyrite provide strong evidence that the formation of sulphur is not by the acid decomposition of thiosulphate. The results presented here and those of Flatt and Woods (1995) are explained by the formation of sulphur and sulphate by independent routes.

(7) Since the oxidation and reduction reactions occur independently, but subject to the mixed potential condition, the electrochemical model described here takes account of the observations that the anodic dissolution is influenced by the electronic structure of pyrite.

REFERENCES

Ahlberg E. and Broo A. E. (1997) Electrochemical reaction mechanisms at pyrite in acidic perchlorate solutions. *J. Electrochem. Soc.* **144,** 1281–1286.

Bailey L. K. and Peters E. (1976) Decomposition of pyrite in acids by pressure leaching and anodization: the case for an electrochemical mechanism. *Can. Metall. Q.* **15,** 333–344.

Biegler T., Rand D. A. J., and Woods R. (1975) Oxygen reduction on sulphide minerals. Part 1. Kinetics and mechanism at rotated pyrite electrodes. *Electroanal. Chem. Int. Electrochem.* **60,** 151–162.

Biegler T. and Swift D. A. (1979) Anodic behaviour of pyrite in acid solutions. *Electrochim. Acta* **24,** 415–420.

Bronold M., Tomm Y., and Jaegermann W. (1994) Surface states on cubic d-band semiconductor pyrite (FeS_2). *Surf. Sci.* **314,** L931–L936.

Bryson L. J. (1999) The contribution of surface states to the anodic dissolution of n-type pyrite (FeS_2) in hydrochloric acid solutions. Personal communication.

Buckley A. N. and Woods R. (1987) The surface oxidation of pyrite. *Appl. Surf. Sci.* **27,** 437–452.

Chen G., Zen J., Fan F., and Bard A. J. (1991) Electrochemical investigation of the energetics of irradiated FeS_2 (pyrite) particles. *J. Phys. Chem.* **95,** 3682–3687.

Crundwell F. K. (1988a) The influence of the electronic structure of solids on the anodic dissolution and leaching of semiconducting sulphide minerals. *Hydrometall.* **21,** 155–190.

Crundwell F. K. (1988b) The influence of iron impurity in zinc sulphide concentrates on the rate of dissolution. *Am. Inst. Chem. Engng. J.* **34,** 1128–1134.

Doyle F. M. and Mirza A. H. (1996) Electrochemical oxidation of pyrite samples with known composition and electrical properties. In *Electrochemistry in Mineral and Metal Processing IV* (eds. F. M. Doyle, P. E. Richardson, and R. Woods), pp. 119–130, The Electrochemical Society.

Evangelou V. P. (1995) *Pyrite Oxidation and Its Control*, p. 293. CRC Press.

Flatt J. R. and Woods R. (1995) A voltammetric investigation of the oxidation of pyrite in nitric acid solutions: relation to treatment of refractory gold ores. *J. Appl. Electrochem.* **25,** 852–856.

Fowler T. A., Holmes P. R., and Crundwell F. K. (1999) The mechanism of the dissolution of pyrite in the presence of Thiobacillus ferrooxidans. *Appl. Environ. Microbiol.* **65,** 2987–2993.

Garrels R. M. and Thompson M. E. (1960) Oxidation of pyrite by iron sulfate solutions. *Aust. J. Sci.* **258**-A, 57–67.

Holmes P. R., Fowler T. A., and Crundwell F. K. (1999) The mechanism of bacterial action in the leaching of pyrite by *Thiobacillus ferrooxidans*: an electrochemical study. *J. Electrochem. Soc.* **146**.

Jaegermann W. and Tributsch H. (1983) Photoelectrochemical reactions of FeS_2 (pyrite) with H_2O and reducing agents. *J. Appl. Electrochem.* **13,** 743–750.

Janz G. J., Coutts J. W., Downey J. R., Jr., and Roduner E. (1976a)

Raman studies of sulfur containing anions in inorganic polysulfides. Potassium polysulfides. *Inorg. Chem.* **15,** 1755–1759.

Janz G. J., Downey J. R., Jr., Roduner E., Wasilczyk G. J., Coutts J. W., and Eluard A. (1976b) Raman studies of sulfur containing anions in inorganic polysulfides. Sodium polysulfides. *Inorg. Chem.* **15,** 1759–1763.

Johnston F. and McAmish L. (1973) A study of the rates of sulfur production in acid thiosulphate solutions using S-35. *J. Colloids Interface Sci.* **42,** 112–119.

Kelsall G. H., Yin Q., Vaughan D. J., England K. E. R. (1996) Electrochemical oxidation of pyrite (FeS$_2$) in acidic aqueous electrolytes I. In *Electrochemistry in Mineral and Metal Processing IV* (eds. F. M. Doyle, P. E. Richardson, and R. Woods) pp. 131–142, The Electrochemical Society.

Li J., Wadsworth M. (1993) Raman spectroscopy of electrochemically oxidized pyrite and optimum conditions for sulfur formation. In *Hydrometallurgy: Fundamentals, Technology and Innovation* (eds. J. B. Hiskey and G. W. Warren), pp. 127–141, SME.

Lowson R. T. (1982) Aqueous oxidation of pyrite by molecular oxygen. *Chem. Rev.* **82,** 461–497.

Luther G. W. III (1987) Pyrite oxidation and reduction: Molecular orbital theory considerations. *Geochim. Cosmochim. Acta* **51,** 3193–3199.

Mathews C. T. and Robins R. G. (1972) The oxidation of ferrous disulfide by ferric sulphate. *Australian Chem. Eng.* **13,** 21–25.

Mathews C. T. and Robins R. G. (1974) Aqueous oxidation of iron disulfide by molecular oxygen. *Australian Chem. Eng.* **15,** 19–24.

McKibben M. A. and Barnes H. L. (1986) Oxidation of pyrite in low temperature acidic solutions: rate laws and surface textures. *Geochim. Cosmochim. Acta* **50,** 1509–1520.

Meyer R. E. (1979) Electrochemistry of FeS$_2$. *J. Electroanaly. Chem.* **101,** 59–71.

Mishra K. K. and Osseo-Asare K. (1988) Aspects of the interfacial electrochemistry of semiconductor pyrite (FeS$_2$). *J. Electrochem. Soc.* **135,** 2502–2509.

Mishra K. K., and Osseo-Asare K. (1992) Electroreduction of Fe^{3+}, O$_2$ and Fe(CN)$_6^{3-}$ at the n-pyrite (FeS$_2$) surface. *J. Electrochem. Soc.* **139,** 3116–3120.

Moses C. O., Nordstrom D. K., Herman J. S., and Mills A. L. (1987) Aqueous pyrite oxidation by dissolved oxygen and ferric ion. *Geochim. Cosmochim. Acta* **51,** 1561–1571.

Moses C. O. and Herman J. S. (1991) Pyrite oxidation at circumneutral pH. *Geochim. Cosmochim. Acta* **55,** 471–482.

Mycroft J. R., Bancroft G. M., McIntyre N. S., Lorimer J. W., and Hill I. R. (1990) Detection of sulphur and polysulphides on electrochemically oxidized pyrite surfaces by X-ray photoelectron spectroscopy and Raman spectroscopy. *J. Electroanal. Chem.* **292,** 139–152.

Nicol M. J., Needes C. S. R., and Finkelstein N. P. (1975) Electrochemical model for the leaching of uranium dioxide. In Leaching and reduction in hydrometallurgy (ed. A. R. Burkin) pp. 1–11, Institute of Mining Metallurgy, London.

Peters E. and Majima H. (1968) Electrochemical reactions of pyrite in acid perchlorate solutions. *Can. Metall. Q.* **7,** 111–117.

Reedy B. J., Beattie J. K., and Lowson R. T. (1991) A vibrational spectroscopic ^{18}O tracer study of pyrite oxidation. *Geochim. Cosmochim. Acta* **55,** 1609–1614.

Salvador P., Tafalla D., Tributsch H., and Wentzel H. (1991) Reaction mechanisms at the FeS$_2$/I interface. *J. Electrochem. Soc.* **138,** 3361–3369.

Schubert B. and Tributsch H. (1990) Photoinduced electron transfer by coordination chemical pathways across pyrite/electrolyte interfaces. *Inorg. Chem.* **29,** 5041–5046.

Shuey R. T. (1975) Semiconducting Ore Minerals. Elsevier.

Singer P. C. and Stumm W. (1970) Acid mine drainage: The rate limiting step. *Science* **167,** 1121–1123.

Smith E. E. and Shumate K. S. (1970) Report by the Ohio State Research Foundation for the Federal Water Pollution Control Administration. Program No. FWPCA, Grant No. 14010, FPS.

Springer (1970) Observations on the electrochemical reactivity of semiconducting minerals. *Trans. Inst. Min. Metall. C* **79,** C11–C15.

Taylor B. E., Wheeler M. C., and Nordstrom D. K. (1984a) Oxygen and sulfur compositions of sulfate in acid mine drainage: Evidence for oxidation mechanisms. *Nature* **308,** 538–541.

Taylor B. E., Wheeler M. C. and Nordstrom D. K. (1984b) Stable isotope geochemistry of acid mine drainage: Experimental oxidation of pyrite. *Geochim. Cosmochim. Acta* **48,** 2669–2678.

Wiersma C. L. and Rimstidt J. D. (1984) Rates of reaction of pyrite and marcasite with ferric ion at pH 2. *Geochim. Cosmochim. Acta* **48,** 85–92.

Williamson M. A. and Rimstidt J. D. (1994) The kinetics and electrochemical rate-determining step of aqueous pyrite oxidation. *Geochim. Cosmochim. Acta* **58,** 5443–5454.